NOTE

Pathology

Feline uterine carcinosarcoma infiltrated with osteoclast-like giant cells

Mami MURAKAMI[1)]*, **Kayoko YONEMARU**[2)], **Minami GOTO**[2)], **Keishi OWAKI**[3)], **Akihiro HIRATA**[2)], **Shoichi KUNIHIRO**[4)], **Hiroki SAKAI**[2,3)]

[1)]Laboratory of Veterinary Clinical Oncology, Faculty of Applied Biological Sciences, Gifu University, Gifu, Japan
[2)]Laboratory of Veterinary Pathology, Faculty of Applied Biological Sciences, Gifu University, Gifu, Japan
[3)]Laboratory of Veterinary Pathology, Joint Graduate School of Veterinary Sciences, Gifu University, Gifu, Japan
[4)]Yodo Animal Hospital, Kyoto, Japan

ABSTRACT. A 12-year-old female Himalayan cat underwent an ovariohysterectomy to remove an intra-abdominal mass. Histologic examination using immunohistochemical staining revealed that the mass was comprised of epithelial and mesenchymal components. Within the lesion, multinucleated giant cells (MGCs) were observed diffusely. MGCs were positive for vimentin and Iba-1 and negative for cytokeratin AE1/AE3 and CD204. In addition, MGCs were negative for Ki-67, indicating nonneoplastic cells. Osteoclast-like MGC (OLMGC) phenotype with tartrate-resistant acid phosphatase positivity was also seen. These findings suggested that the uterine tumor was carcinosarcoma with OLMGCs. Uterine tumors in humans, such as leiomyosarcoma and carcinosarcoma, with OLMGC infiltration, are well-known pathologic entities; however, they are rare in animals and to our knowledge, have not been previously reported in cats.

KEYWORDS: carcinosarcoma, feline, osteoclasts, ovariohysterectomy, uterine tumor

Uterine neoplasms are rare in cats and account for only 0.29% of all neoplastic diseases [20]. Adenocarcinoma is the most common uterine tumor in cats; other uterine neoplasms include Müllerian tumors (adenosarcoma), leiomyoma, leiomyosarcoma, fibrosarcoma, and lymphoma [12, 20].

In human medicine, uterine carcinosarcoma (UCS) and malignant mixed Müllerian tumor were synonymous in the previous WHO classification; however, the current WHO classification considers these tumors to be different from malignant mixed Müllerian tumors and carcinosarcomas [17, 25]. Feline UCS is composed of both epithelial and mesenchymal components [15, 18]. To our knowledge, feline UCS with osteoclast-like multinucleated giant cells (OLMGCs) has not been reported previously. Based on the information in scientific literature databases (i.e., Medline, Scopus, Web of Science), an association of UCS infiltrated with osteoclast-like giant cells has not been reported in any veterinary species.

A 12-year-old anorectic female Himalayan cat was admitted to a private veterinary clinic. Hematologic tests revealed no abnormalities. Abdominal palpation suggested a mass that, through abdominal radiography, was located in the uterus. Thoracic radiography revealed a pulmonary nodule suspicious of metastasis (Fig. 1A). Two days later, the abdominal mass was removed through laparotomy, which resulted in an ovariohysterectomy because the mass was located from the base to the middle of the uterine horn. No macroscopic evidence of intraperitoneal dissemination or lymph node metastasis was observed, even though the enlarged right uterine horn adhered to the greater omentum. The resected uterine cavity was filled with fluid and dilated to 12.8 × 5.6 cm; the mass was white and firm (Fig. 1B).

The uterine mass was fixed in 10% neutral-buffered formalin. A gross examination of the formalin-fixed mass revealed that the mass had grown exophytically. It was gray-white speckled with several yellow foci on the cut surface (Fig. 1C). Samples were processed routinely, and sections were stained with H&E. Immunohistochemical analysis was performed (Universal immuno-enzyme polymer method, simple stain MAX PO; Nichirei Biosciences, Tokyo, Japan) with primary antibodies (Table 1). The specimens were deparaffinized and rehydrated using graded alcohol. Endogenous peroxidase activity was quenched using 0.3% H_2O_2, followed by heat-induced antigen retrieval in an autoclave with active pH 6.0 (Immuneactive; Matsunami Glass Industry, Osaka, Japan). Thereafter, the sections were treated with blocking buffer (Protein block serum-free; Dako, Tokyo, Japan) for 10 min and were incubated with the primary antibody overnight at 4°C. The sections were washed and treated with the corresponding secondary antibodies (Histofine® Simple Stain MAX PO (M), Histofine® Simple Stain MAX PO (R), Nichirei Biosciences). Thereafter, the sections were treated with
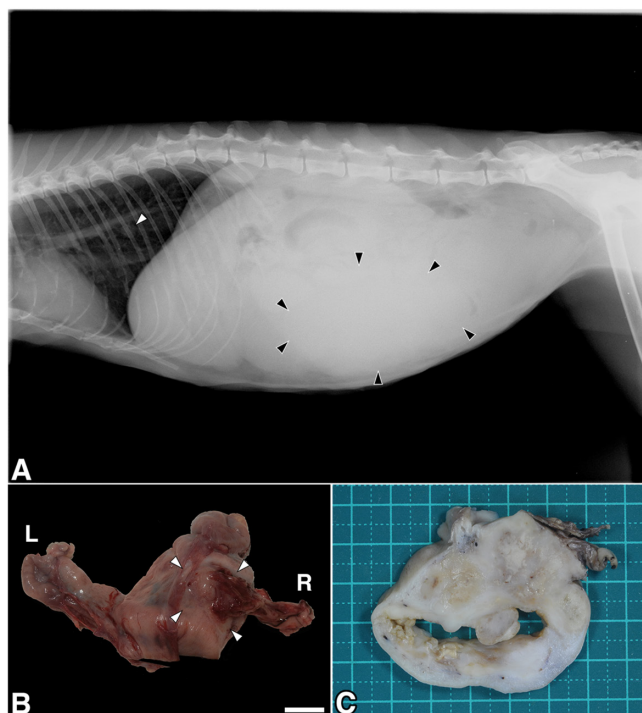
Fig. 1. Radiographic and gross images of feline uterine carcinosarcoma. (**A**) Radiographic image of the mass in the abdominal cavity (black arrowheads). A lung nodule was detected (white arrowhead). (**B**) Gross appearance of the uterine lesion. The mass was observed in the proximal part of the right uterine horn (white arrowhead). (**C**) Cut surface of the tumor. Gray-white mottled appearance with several yellow foci scattered throughout the tumor parenchyma.

Table 1. Summary and results of Immunohistochemistry

Antibody	Clone	Source	Dilution	Antigen retrieval	Source	Staining results		
						Epithelial components	Mesenchymal components	OLGLs*
Cytokeratin	AE1/AE3	Mouse	1:10	121°C 15 min Autoclave pH6.0	Dako Japan	++	+/−	−
Vimentin	V9	Mouse	1:10	121°C 15 min Autoclave pH6.0	Nichirei Biosciences	+/−	++	−
Desmin	D33	Mouse	1:5	121°C 15 min Autoclave pH6.0	Dako Japan	−	+/−	−
α-smooth muscle actin	1A4	Mouse	1:5	121°C 15 min Autoclave pH6.0	Dako Denmark	−	++	−
E-cadherin	36	Mouse	1:200	121°C 15 min Autoclave pH6.0	BD Transduction Laboratories	++	+/−	−
CD204	SRA-E5	Mouse	1:800	121°C 15 min Autoclave pH6.0	Trans Genic Inc.	−	−	−
Ki-67	MIB-1	Mouse	1:50	121°C 15 min Autoclave pH6.0	Dako Denmark	++	++	−
Iba-1	Polyclonal	Rabbit	1:500	121°C 15 min Autoclave pH6.0	FUJIFILM Wako Chemicals Corp.	−	−	+

Dako Denmark (Glostrup, Hovedstaden, Denmark), BD Transduction Laboratories (Franklin Lakes, NJ, USA), Trans Genic Inc. (Kobe, Japan), FUJIFILM Wako Chemicals Corp. (Osaka, Japan). All antibodies were treated with 121°C 15 min in an autoclave for antigen retrieval. *OLGLs; osteoclast-like multinucleated giant cells. ++= >50% of the cells stained positive; +=10–50% of the cells stained positive; +/−= <10% of the cells stained positive; −negative.

3,3′-diaminobenzidine as a chromogen and were counterstained with hematoxylin. To further characterize the multinucleated giant cells (MGCs), 2-μm-thick sections were stained with tartrate-resistant acid phosphatase (TRAP TRAP/ALP stain kit; Wako Pure Chemical, Tokyo, Japan). The deparaffinized and rehydrated tissue sections were incubated at room temperature (25°C) in acetate-tartaric acid buffer (pH 5.0) for 25 min. The sections were then washed using distilled water and were counterstained using aqueous hematoxylin.

Histologic examination revealed that the tumor had indistinct margins and growth beyond the endometrium with the proliferation of carcinomatous and sarcomatous components. Some areas contained a mixture of both components; however, the predominant site of each component was found in the tumor tissue (Fig. 2). There was no expansive growth beyond the serosa. The epithelial components formed irregular tubular, alveolar structures, or solitary proliferated, and the sarcomatous components were arranged in irregular bundles of spindle cells. Both components of the tumor cells were cuboidal-to-polygonal with moderate amounts of eosinophilic cytoplasm containing variably sized nuclei with distinct nucleoli. Furthermore, both components of tumor cells contained atypical nuclei and variable amounts of cytoplasm. Necrotic regions occurred mainly in the sarcomatous area and were surrounded by neutrophils. The total mitotic count was 29 in the epithelial component and 44 in the sarcomatous component (ten 40× hpf fields, 2.37 mm^2). The atypical mitotic count was 1 in the carcinomatous component and 2 in the sarcomatous component. In addition, MGCs were distributed throughout the tumor, especially in the sarcomatous component (Fig. 4A). MGCs appeared adjacent to areas of necrotic foci or degenerate muscle fibers that were included in tumor tissue, but were also seen elsewhere in the tumor. They contained a large
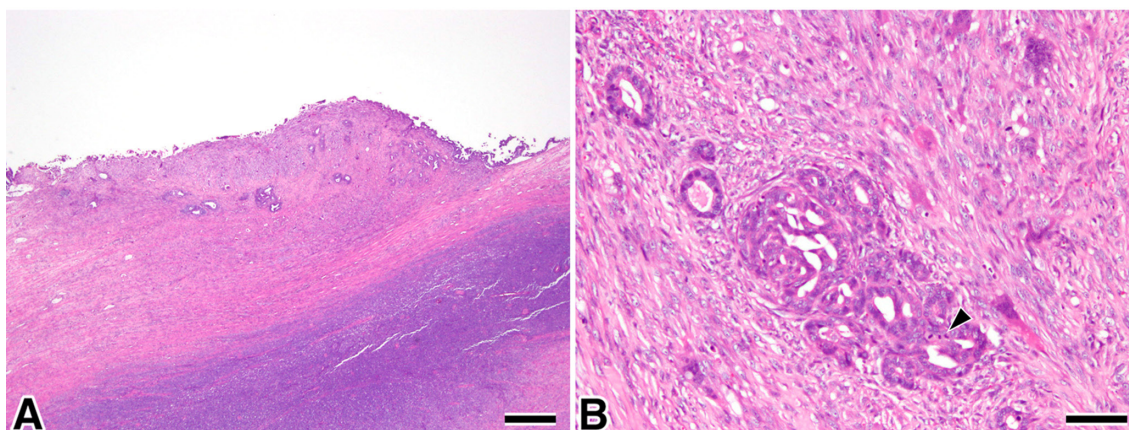
Fig. 2. Histologic characteristics of the feline uterine carcinosarcoma. H&E. (**A**) the tumor had indistinct margins and growth beyond the endometrium, with the proliferation of carcinomatous and sarcomatous components. Both components mixed in some areas, however, the predominant site of each component was found in the tumor tissue. The left part shows the area with the predominantly sarcomatous component, and the right part shows the area with the predominantly epithelial component. (**B**) The epithelial-derived tumor cells, showing irregular luminal shapes of various sizes, had round nuclei and moderate-to-small amounts of eosinophilic cytoplasm. Nucleoli were distinct, and nuclear size was variable. The sarcoma component proliferated in bundles. A mitotic image was also observed (black arrowheads). (A) Bar=500 μm, (B) Bar=25 μm.

number of partially superimposed pale nuclei (some with prominent nucleoli), clustered in the center of the cytoplasm. The tumor did not extend into the endocervical stroma or mucosa, and the regional lymph nodes showed no evidence of metastasis.

Cytokeratin (CK) AE1/AE3 was expressed strongly, whereas E-cadherin and vimentin were expressed at variable levels from weak to strong in the epithelial component forming the tubular structure (Fig. 3A, 3B, 3E). Most of the sarcomatous component was strongly immunolabeled with vimentin (Fig. 3B) and α-smooth muscle actin (SMA) (Fig. 3D), in contrast to the very few positive observations of CK AE1/AE3 (Fig. 3A), desmin (Fig. 3C), and E-cadherin (Fig. 3E). In addition, most of the sarcomatous components showed weak, positive cytoplasmic immunolabeling for calponin (Fig. 3F). The Ki-67 positive index (Ki-67 PI) for the epithelial component was 41.0% and for the sarcomatous components was 56.4%.

As for MGCs, strong positive immunolabeling was detected for ionized calcium-binding adaptor molecule 1 (Iba-1), an identical protein to Iba1 as well as vimentin (Fig. 4B, 4E), and a negative reaction was detected regarding CD204, α-SMA, CK AE1/AE3, and Ki-67 in MGCs (Fig. 4C, 4D, 4F, and 4G). TRAP analysis revealed the presence of TRAP-positive material in the cytoplasm of most MGCs and some macrophages (Fig. 4H). However, some of the MGCs were TRAP-negative. The diagnosis of UCS with infiltrated OLMGCs was made based on a mixture of epithelial and mesenchymal components and infiltration of TRAP-positive MGCs into the tumor.

Although the cat's condition improved without chemotherapy or any other treatment after surgery, a follow-up examination 2 months after surgery revealed a recurrence of the tumor and an increase in the number and size of pulmonary metastatic lesions (Fig. 5). The cat died of clinical worsening, including anorexia soon after the 2 months follow-up, which may be thought to have fallen into cachexia. No postmortem examination was performed.

Although very few sarcomatous components showed positive immunohistochemical staining for CK AE1/AE3, which is pan CK, and E-cadherin, tissue conversion between epithelial and sarcomatous components is not clear. However, both carcinoma and sarcomatous components were observed in the present case, which was consistent with the definition of a biphasic tumor composed of carcinomatous and sarcomatous components for carcinosarcoma. Therefore, this case was diagnosed as carcinosarcoma [17].

Carcinosarcoma has been reported in cats, predominantly in the uterus, lungs, thyroid, pancreas, biliary system, and mammary glands [4, 7, 8, 15, 18, 19, 28]. The histogenesis of carcinosarcoma is not comprehensively understood; four major theories have been proposed (i.e., the collision, association, conversion, and composition theories). In human medicine, the most accepted theory is that of conversion, which claims that UCS originates from the metamorphosis of a single cell [3]. The conversion theory is supported by data such as similar chromosomal aberrations, cytogenic aspects, concordant loss of heterozygosity, and identical *p53/Kras* mutations [3]. Moreover, UCS cells have phenotypic plasticity regarding epithelial-mesenchymal transition (EMT) and mesenchymal-epithelial transition [9]. The immunophenotype of sarcomatous components differs between studies regarding nonperformance of immunostaining, vimentin positivity, and α-SMA and/or desmin negativity [8, 19, 28]. In our case, the immunophenotype of the sarcomatous component likely differed from those reported previously since most of the sarcomatous cells were negative for desmin and positive for α-SMA and weakly positive for calponin. Calponin is expressed in well-differentiated smooth muscle, myoepithelial cells such as mammary gland and salivary gland cells, and in myofibroblasts, suggesting that the sarcomatous cells of our case were differentiated into myofibroblastic cells. Tumor cells with EMT have been reported to express α-SMA, which may explain why many of the sarcomatous cells in our case had a myofibroblast-like phenotype [9, 16].

Furthermore, the epithelial components formed the alveolar structure, and solitary proliferation was observed. In addition, the high N/C ratio, the high number of mitotic figures, and the high Ki-67 PI indicate the malignant nature. In this case, the malignant
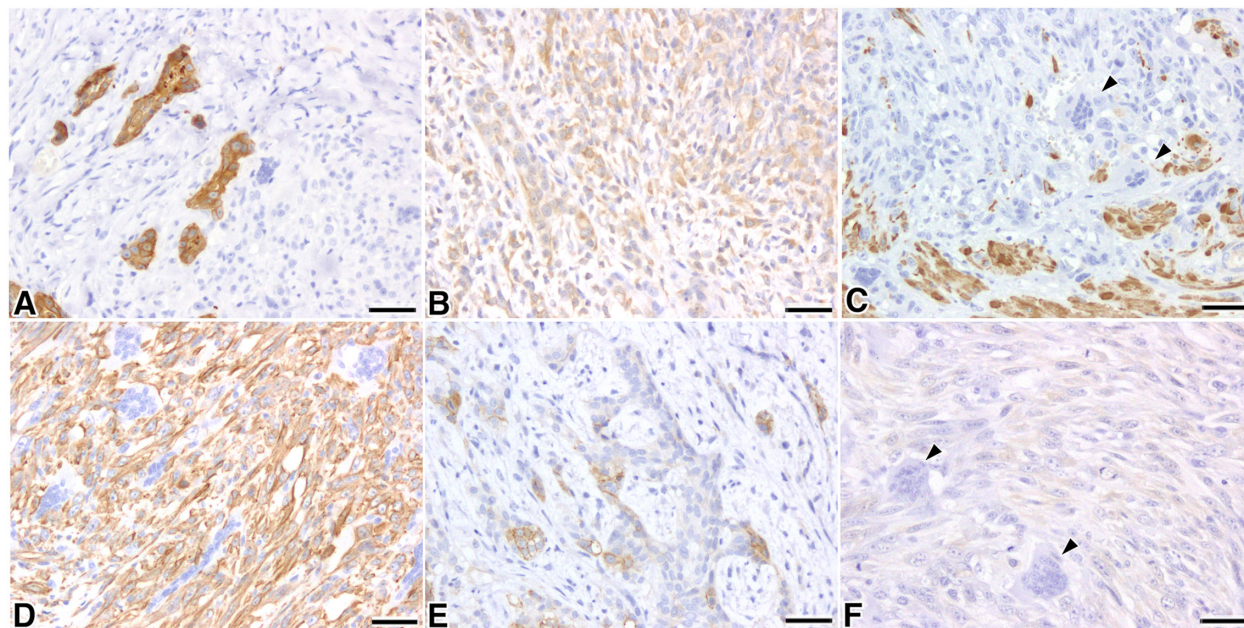
Fig. 3. Immunohistologic characteristics of the feline uterine carcinosarcoma. Immunohistochemistry; chromogen: 3,3′-diaminobenzidine, hematoxylin counterstain. (**A**) Intense cytoplasmic positive immunolabeling for CK AE1/AE3 within carcinomatous cells, whereas sarcomatous components showed negative immunolabeling. (**B**) Intense positive cytoplasmic immunolabeling for vimentin within both carcinomatous cells and sarcomatous components. (**C**) Desmin expression in sarcomatous components. Most of the sarcomatous cells were negative, while positive immunolabeling in the cells in the muscle layer was detected. Multinucleate giant cells (MGCs) showed negative immunolabeling (black arrowheads). (**D**) Positive immunolabeling for α-smooth muscle actin in sarcomatous components. (**E**) E-cadherin showed positive immunolabeling in many epithelial component tumor cells, but some showed weaker positive immunolabeling. On the other hand, sarcomatous components showed negative or weak immunolabeling for E-cadherin. (**F**) Calponin expression in sarcomatous components. Most of the sarcomatous components showed cytoplasmic weak positive immunolabeling. MGCs showed negative immunolabeling (black arrowheads). Bars=25 μm.
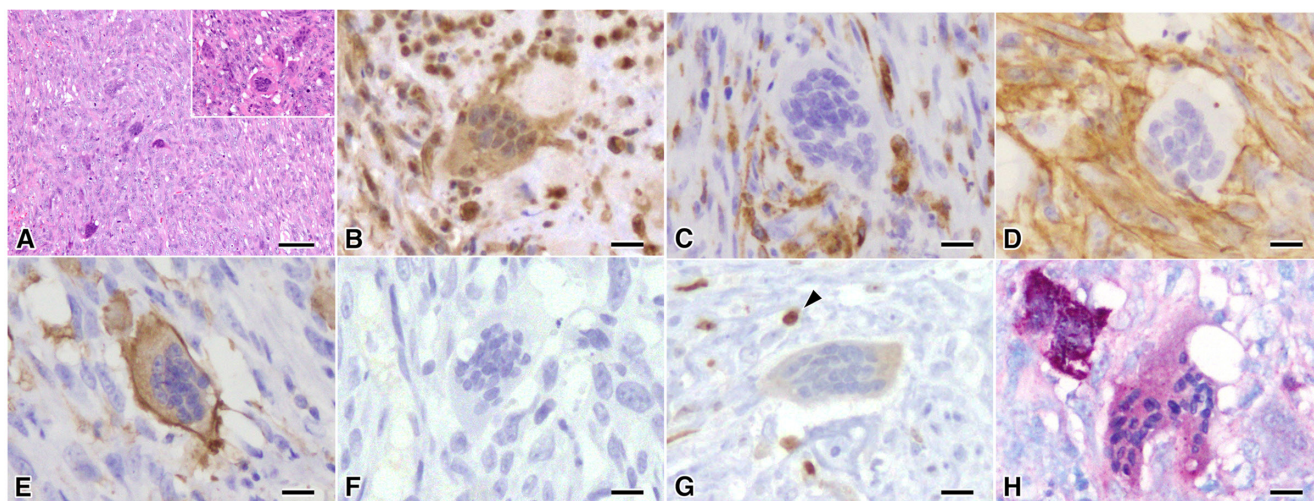

Fig. 4. Histologic, immunohistologic features and tartrate-resistant acid phosphatase (TRAP) stain of multinucleate giant cells (MGCs) in a feline uterine carcinosarcoma. Immunohistochemistry; chromogen: 3,3′-diaminobenzidine, hematoxylin counterstain. (**A**) MGCs containing 20–30 nuclei (inset) with oval grooved, vesicular nuclei and small nucleoli scattered among the sarcomatous spindle cells. H&E. (**B**) Positive immunolabeling for vimentin in an MGC. (**C**) Negative immunolabeling for CD204 (SRA) in an MGC. Macrophages as an internal control (black arrowhead). (**D**) Negative immunolabeling for α-smooth muscle actin in an MGC. (**E**) Positive cytoplasmic immunolabeling for Iba1/AIF-1 in an MGC. (**F**) Negative immunolabeling for CK AE1/AE3 in an MGC. (**G**) Negative immunolabeling for Ki-67 in an MGC. Positive internal control (black arrowhead). (**H**) MGCs had strong positive cytoplasmic reactivity for TRAP. (A); Bar=50 μm, (B)–(H); Bars=10 μm.
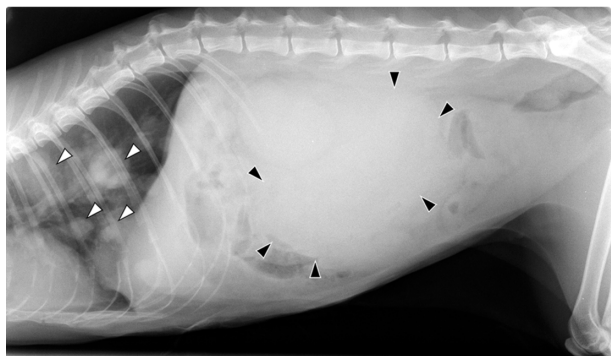
Fig. 5. Radiographic image of feline uterine carcinosarcoma. Radiographic image of the recurred mass in the abdominal cavity (black arrowheads). The number and the size of lung nodules were increased to compare to the first visit (white arrowheads).

mesenchymal component was the predominant component, but a small number of malignant proliferating epithelial components were observed, which led to the diagnosis of carcinosarcoma. Furthermore, the two malignant elements were present, suggesting that this case differs from Sato *et al.* [21].

Particularly intriguing in our case were the numerous MGCs in the tumor. Giant cells can infiltrate several neoplasms in cats, such as malignant giant cell tumors and fibrosarcoma, and osteoclast-like giant cell tumors have also been reported in cats [5, 6]. In contrast to neoplastic MGCs, the absence of MCGs with nuclear positivity for Ki-67 (MIB1) in immunostaining also supports the assumption that MGCs in our case were not neoplastic. MGCs in our case had negative immunoreactivity for cytokeratin AE1/AE3, α-SMA, and desmin, suggesting that these MGCs were not derived from the sarcomatous and epithelial components of the tumor.

MGCs in our case expressed an osteoclast phenotype, indicated by TRAP positivity. TRAP is synthesized and secreted by osteoclasts and in the process in which hematopoietic mononuclear progenitor cells of osteoclasts into multinucleated osteoclasts by cell fusion [13]. In addition, it has been reported that M1/M2 macrophages that have acquired osteoclastogenic potential also show TRAP positivity [27]. Thus, TRAP is a reliable indicator of osteoclasts.

Iba1, a marker of activated macrophages and microglia and CD204, is preferentially expressed in immune cells of the myeloid lineage, including dendritic cells and macrophages. CD204, also known as a class A scavenger receptor (SRA) or macrophage scavenger receptor, is a prototypical member of a family of structurally diverse transmembrane receptors, collectively termed scavenger receptors. In addition, during osteoclast maturation, mononuclear osteoclasts express CD204/SRA, whereas CD204/SRA expression decreases or disappears after differentiating into mature multinucleated osteoclasts [23]. TRAP-positive reactivity and CD204/SRA-negative reactivity in MGCs in our case support the identification of mature OLMGCs [1].

In human medicine, CD68/KP-1 (a marker of various cells of macrophage lineage, including monocytes, histiocytes, giant cells, Kupffer cells, and osteoclasts) immunoexpression identifies OLMGCs in tumors [22]. However, cross-reactivity with CD68 was not observed in our case (data not shown).

In tumors of the human uterus, GC infiltration has been reported in both endometrial and mesenchymal tumors, especially leiomyosarcomas, in tumors arising in the human uterus [2, 9–11, 14, 22, 24]. Infiltrated OLMGCs are sometimes observed in human uterine leiomyosarcoma with intralesional mineralization and in tumor tissues without calcium deposition [10]. In our case, calcareous deposition was not observed, not even in necrotic foci.

Although the prognosis for human UCS with GC invasion is unknown, the prognosis for UCS is worse than that for usual endometrial adenocarcinomas, with a reported 5-year survival rate of about 30%. Such tumors with GC invasion of the uterus have often only been reported in case reports and include stages I-IV with prognoses ranging from 15 to 168 months; thus, the prognosis is not fully known [14].

Mulligan *et al.* reviewed uterine tumors with GC infiltration in women, summarizing five cases and reviewing previous papers [14]. They described that the paucity of case reports has been associated with the possible classification of other tumors, such as malignant fibrous histiocytosis, the misclassification of GC infiltration as one of the other endometrial cancer subtypes that may be characterized by GC or pleomorphic elements, and the lack of definitions and guidelines to facilitate accurate and reproducible classification of these tumors. In addition, they defined the tumor with giant cell invasion based on the WHO classification at that time and the spectrum of lung cancer, and at the same time, developed an algorithm [14].

The algorithm first classifies tumors as benign or malignant. When malignant, (1) When dealing with cancer, it is determined if the giant cell is epithelial or malignant, a specific cell type is identified, and it is determined whether the giant cell exists >10% or whether the malignant stromal component exists. Afterward, it is diagnosed as mixed carcinoma: Usual carcinoma with giant cell carcinoma component, type according to usual elements but mention the presence of the giant cell component, or carcinosarcoma. (2) When osteoclast-like giant cells are infiltrated, whether other malignant mesenchymal elements are included or not is judged, and then it is diagnosed as malignant giant cell tumor, leiomyosarcoma with OLGC, undifferentiated sarcoma with OLGC, and endometrial stromal neoplasm with OLGC. (3) When trophoblastic giant cells appear, whether the component of typical epithelial cancer exists or not is judged, and it is diagnosed as choriocarcinoma, endometrial carcinoma with scattered trophoblastic giant cells, or endometrial carcinoma with frank choriocarcinomatous differentiation [14].

According to the algorithm, this case does not correspond to either. However, as far as we know, there is only one case report of carcinosarcoma of the uterus with giant cell invasion in humans [2], and there is no description of the invasion of the MGCs in any of the feline carcinosarcoma reports. Since the MGC invasion of this case seems to be characteristic, it was better to be included in the diagnosis. In addition, since it was revealed that the MGCs of this case had the feature osteoclast-like, we can appropriately hypothesize this case is carcinosarcoma with OLMGC.

Expression of receptor activator of nuclear factor kappa-B ligand, which is expressed on the cell membrane of osteoblasts and acts through intercellular adhesion, has been detected in infiltrated OLMGCs of human leiomyosarcomas [24]. This suggests that

OLMGCs are differentiated in tumors in a manner similar to osteoclast differentiation in bone [24]. In addition, dendritic cell–specific transmembrane protein has been reported to induce cell fusion in macrophages, leading to differentiation from macrophages into either osteoclasts or foreign body giant cells [26]. This mechanism may be involved in the presence of TRAP-negative giant cells in our case. However, the mechanism of infiltration of OLMGCs in tumors is unclear. Further cases of malignant tumors associated with OLMGC infiltration are required to investigate their behavior.

CONFLICT OF INTEREST. The authors declare no potential conflicts of interest with respect to the research, authorship, and/or publication of this manuscript.

REFERENCES

1. Ahmed GJ, Tatsukawa E, Morishita K, Shibata Y, Suehiro F, Kamitakahara M, Yokoi T, Koji T, Umeda M, Nishimura M, Ikeda T. 2016. Regulation and biological significance of formation of osteoclasts and foreign body giant cells in an extraskeletal implantation model. *Acta Histochem Cytochem* **49**: 97–107. [Medline] [CrossRef]
2. Amant F, Vandenput I, Van Gorp T, Vergote I, Moerman P. 2006. Endometrial carcinosarcoma with osteoclast-like giant cells. *Eur J Gynaecol Oncol* **27**: 92–94. [Medline]
3. Cantrell LA, Blank SV, Duska LR. 2015. Uterine carcinosarcoma: a review of the literature. *Gynecol Oncol* **137**: 581–588. [Medline] [CrossRef]
4. Cavicchioli L, Ferro S, Callegari C, Auriemma E, Zini E, Zappulli V. 2013. Carcinosarcoma of the biliary system in a cat. *J Vet Diagn Invest* **25**: 562–565. [Medline] [CrossRef]
5. Chang SC, Liao JW, Liu CI, Wong ML, Cheng FP. 2008. Osteoclastic-like giant cell tumour in a cat. *J Feline Med Surg* **10**: 403–406. [Medline] [CrossRef]
6. Couto SS, Griffey SM, Duarte PC, Madewell BR. 2002. Feline vaccine-associated fibrosarcoma: morphologic distinctions. *Vet Pathol* **39**: 33–41. [Medline] [CrossRef]
7. Fusaro L, Panarese S, Brunetti B, Zambelli D, Benazzi C, Sarli G. 2009. Quantitative analysis of telomerase in feline mammary tissues. *J Vet Diagn Invest* **21**: 369–373. [Medline] [CrossRef]
8. Ghisleni G, Grieco V, Mazzotti M, Caniatti M, Roccabianca P, Scanziani E. 2003. Pulmonary carcinosarcoma in a cat. *J Vet Diagn Invest* **15**: 170–173. [Medline] [CrossRef]
9. Kalluri R, Weinberg RA. 2009. The basics of epithelial-mesenchymal transition. *J Clin Invest* **119**: 1420–1428. [Medline] [CrossRef]
10. Manglik N, Sawicki J, Saad A, Fadare O, Soslow R, Liang SX. 2012. Giant cell tumor of uterus resembling osseous giant cell tumor: case report and review of literature. *Int J Surg Pathol* **20**: 618–622. [Medline] [CrossRef]
11. Marshall RJ, Braye SG, Jones DB. 1986. Leiomyosarcoma of the uterus with giant cells resembling osteoclasts. *Int J Gynecol Pathol* **5**: 260–268. [Medline] [CrossRef]
12. Miller MA, Ramos-Vara JA, Dickerson MF, Johnson GC, Pace LW, Kreeger JM, Turnquist SE, Turk JR. 2003. Uterine neoplasia in 13 cats. *J Vet Diagn Invest* **15**: 515–522. [Medline] [CrossRef]
13. Minkin C. 1982. Bone acid phosphatase: tartrate-resistant acid phosphatase as a marker of osteoclast function. *Calcif Tissue Int* **34**: 285–290. [Medline] [CrossRef]
14. Mulligan AM, Plotkin A, Rouzbahman M, Soslow RA, Gilks CB, Clarke BA. 2010. Endometrial giant cell carcinoma: a case series and review of the spectrum of endometrial neoplasms containing giant cells. *Am J Surg Pathol* **34**: 1132–1138. [Medline] [CrossRef]
15. Nicòtina PA, Zanghì A, Catone G. 2002. Uterine malignant mixed Müllerian tumor (Metaplasic carcinoma) in the cat: clinicopathologic features and proliferation indices. *Vet Pathol* **39**: 158–160. [Medline] [CrossRef]
16. O'Connor JW, Mistry K, Detweiler D, Wang C, Gomez EW. 2016. Cell-cell contact and matrix adhesion promote αSMA expression during TGFβ1-induced epithelial-myofibroblast transition via Notch and MRTF-A. *Sci Rep* **6**: 26226 [CrossRef]. [Medline]
17. Palacios J, Ali-Fehmi R, Carlson JW. 2020. Carcinosarcoma of the uterine corpus. pp. 265–267. In: World Health Organization classification of Female Genital Tumours, 5th ed. (WHO Classification of Tumours Editorial Board eds.), International Agency for Research on Cancer, Lyon.
18. Papparella S, Roperto F. 1984. Spontaneous uterine tumors in three cats. *Vet Pathol* **21**: 257–258. [Medline] [CrossRef]
19. Rich AF, Piviani M, Swales H, Finotello R, Blundell R. 2019. Bilateral thyroid carcinosarcoma in a cat. *J Comp Pathol* **171**: 24–29. [Medline] [CrossRef]
20. Saba CF, Lawrence JA. 2020. Tumors of the female reproductive system. pp. 597–603. In: Withrow and MacEwen's Small Animal Clinical Oncology, 6th ed. (Vail DM, Thamm DH, Liptak LM eds.), Elsevier, Amsterdam.
21. Sato T, Maeda H, Suzuki A, Shibuya H, Sakata A, Shirai W. 2007. Endometrial stromal sarcoma with smooth muscle and glandular differentiation of the feline uterus. *Vet Pathol* **44**: 379–382. [Medline] [CrossRef]
22. Skubitz KM, Manivel JC. 2007. Giant cell tumor of the uterus: case report and response to chemotherapy. *BMC Cancer* **7**: 46. [Medline] [CrossRef]
23. Takemura K, Sakashita N, Fujiwara Y, Komohara Y, Lei X, Ohnishi K, Suzuki H, Kodama T, Mizuta H, Takeya M. 2010. Class A scavenger receptor promotes osteoclast differentiation via the enhanced expression of receptor activator of NF-kappaB (RANK). *Biochem Biophys Res Commun* **391**: 1675–1680. [Medline] [CrossRef]
24. Terasaki M, Terasaki Y, Yoneyama K, Kuwahara N, Wakamatsu K, Nagahama K, Kunugi S, Takeshita T, Shimizu A. 2015. Uterine leiomyosarcoma with osteoclast-like giant cells associated with high expression of receptor activator of nuclear factor κB ligand. *Hum Pathol* **46**: 1679–1684. [Medline] [CrossRef]
25. Wells M, Palacios J, Oliva E, Prat J. 2014. Mixed epithelial and mesenchymal tumours. pp. 148–151. In: World Health Organization classification of Female Reproductive Organs, 4th ed. (Kurman RJ, Carcangiu ML, Herrington CS, Young RH eds.), International Agency for Research on Cancer, Lyon.
26. Yagi M, Miyamoto T, Sawatani Y, Iwamoto K, Hosogane N, Fujita N, Morita K, Ninomiya K, Suzuki T, Miyamoto K, Oike Y, Takeya M, Toyama Y, Suda T. 2005. DC-STAMP is essential for cell-cell fusion in osteoclasts and foreign body giant cells. *J Exp Med* **202**: 345–351. [Medline] [CrossRef]
27. Yamaguchi T, Movila A, Kataoka S, Wisitrasameewong W, Ruiz Torruella M, Murakoshi M, Murakami S, Kawai T. 2016. Proinflammatory M1 macrophages Inhibit RANKL-induced osteoclastogenesis. *Infect Immun* **84**: 2802–2812. [Medline] [CrossRef]
28. Yamamoto R, Suzuki K, Uchida K, Onda N, Shibutani M, Mitsumori K. 2012. Pancreatic carcinosarcoma in a cat. *J Comp Pathol* **147**: 223–226. [Medline] [CrossRef]